

# **Artemisinin as Potential Anticancer Agents: Uptake Detection in Erythrocytes Using Fourier Transform Infrared Spectroscopy and Cytotoxicity against Bladder Cancer Cells**

<sup>1</sup>Charlotte Humphreys, <sup>1</sup>Alan J. Cooper, <sup>1</sup>Eugen Barbu, <sup>2</sup>Brian R. Birch, <sup>3</sup>Bashir A. Lwaleed

1. School of Pharmacy and Biomedical Sciences, Portsmouth University, Portsmouth, UK
2. Department of Urology, University Hospital Southampton NHS Foundation Trust, Southampton, UK
3. Faculty of Health Sciences, University of Southampton, Southampton, UK

## **Corresponding author:**

Dr Bashir A. Lwaleed  
Faculty of Health Sciences  
University of Southampton  
South Academic and Pathology Block (MP 11)  
Southampton General Hospital  
Tremona Road  
Southampton  
SO16 6YD  
United Kingdom

Tel: (+44) 02381 206559

Fax: (+44) 02381 206922

E-mail: [bashir@soton.ac.uk](mailto:bashir@soton.ac.uk)

**Key words:** Artemisinin; Anticancer Agents; Fourier Transform Infrared; Erythrocytes; Cytotoxicity; Bladder Cancer

**Word count:** 2312

## ABSTRACT

**Aims** Semi-synthetic derivatives of the anti-malarial drug artemisinin may also possess anti-cancer properties. The ability to detect artemisinin uptake and distribution in cells would facilitate live cell imaging without labelling. This study describes mid-range infrared absorption spectra for three artemisinin variants and attempts to detect their presence in a simple cell model (erythrocytes). Cytotoxicity assays assess potential anti-cancer properties against bladder cancer cells.

**Methods** Mid-range Fourier transform infrared spectra were obtained from dry preparations of Dihydroartemisinin (DHA), Artesunate (ART) and Artemether (ARTE). Erythrocytes were prepared from normal blood and incubated for 30 minutes at 37°C with the three artemisinin derivatives. Cytospin preparations were prepared on aluminium foil for spectroscopy. Potential for growth inhibition in the RT112 bladder carcinoma cell line was assessed by the 3-(4,5-Dimethylthiazol-2-yl)-2,5-Diphenyltetrazolium Bromide residual viable biomass method.

**Results** Spectra were obtained from the three native compounds. Repeat scans after 8 weeks showed ART and ARTE to be stable, stored under manufacturer's recommendations. DHA exhibited marked changes over the same period. It was possible by subtraction to detect DHA in cytospins, but not ART or ARTE. The fit between the subtraction spectrum and that of the native compound was >80%. DHA and ART showed strong cytotoxic potential against RT112 cells.

**Conclusion** The artemisinin derivatives tested exhibit unique mid-range infrared absorption spectra which can be used to monitor degradation and, for DHA, can be detected by subtraction in loaded erythrocytes rendering future imaging studies feasible. Its cytotoxic efficacy against RT112 cells suggest bladder cancer as a possible target disease.

## WHAT THE PAPER ADDS

The spectra have been added to databases where they had not previously been represented. The ability to detect dihydroartemisinin in erythrocytes by Fourier transform infrared methodology is a step towards imaging studies in live cells that would expand options for tracking the compound in its native state, without the disadvantages of labelling. The demonstration of cytotoxicity against bladder cancer cells is original and enhances the relevance of the study.

## INTRODUCTION

Artemisinin is derived from the sweet wormwood plant *Artemisia annua L* and has a long history of use in Chinese medicine to treat febrile conditions [1]. It is a key component of the World Health Organisation's global anti-malaria strategy, its derivatives representing a class of highly potent anti-malarial drugs. Following success against malaria, originally under the Chinese name, Qinghaosu [2] and subsequently as artemisinin [3], researchers began investigating whether artemisinins held potential anticancer properties. Early reports demonstrating that artemisinins were cytotoxic to tumour cells include experiments with neuronal cells [4] and a range of cancer cells [5]. Subsequent studies have demonstrated, growth inhibition, increased levels of oxidative stress, enhanced apoptosis and inhibition of angiogenesis on exposure to these drugs [6-8]. Some of these properties and mechanisms are outlined below.

Artemisinins are lipophilic and can cross erythrocytic, parasitic and host cell plasma membranes [9] as well as cytoplasmic membrane bound organelles such as mitochondria [10]. The mechanism of artemisinins' activity is known to be dependent upon the  $Fe^{2+}$  mediated oxidization of the atypical endoperoxide bridge [11]. In nucleate cells artemisinins induce apoptosis by a ROS mediated activation loop among caspases 8 and 9 [12] and, optionally also caspase 3 [13]. Semi-synthetic artemisinin derivatives have been formulated to increase solubility and bioavailability *in-vivo*. However, artemisinins are metabolised quickly, so while their rapid activity makes them effective against malaria, the use of artemisinin for cancer treatment/anti-angiogenesis treatment may be limited by its fast elimination from blood plasma, unless slow-release or combination strategies [14] can be developed.

Current malarial therapies and investigations into potential anti-cancer properties are based on the derivatives Dihydroartemisinin (DHA), Artesunate (ART) and Artemether (ARTE) [15]. An aid to research in this area would be an ability to image cellular uptake and distribution in real time, as demonstrated with fluorescence labeling [10]. This prompted us to design a laboratory-based study investigating artemisinin identification by Fourier transform infrared (FT-IR) spectroscopy, offering a label-free reporting system. These initial studies use a relatively simple erythrocyte model, but may represent the beginning of a body of work that ultimately facilitates live cell FT-IR imaging of neoplastic epithelial cells treated with native artemisinin derivatives, enabling a clearer understanding of their uptake, trafficking and metabolism and hence their potential value as adjuvant components of targeted cancer therapies.

## **MATERIALS AND METHODS**

### **In vitro analysis of raw materials**

DHA was packaged in foil and stored below 5°C according to the manufacturer's instructions. The ART and ARTE derivatives were indicated for storage in plastic at room temperature. FT-IR spectroscopy was conducted for each artemisinin derivative using a FT-IR Nexus analyser (Thermo Nicolet, USA) and interpreted by OMNIC (version 6.1) software. A background signal was collected and subtracted from sample signatures. For analysis of the compounds *ex-vivo*, enough crystals to adequately cover the diamond within the sample inlet were held securely in place by a metal clamp. A spectrum was acquired on screen within one minute. The resultant plots showed the absorption and wave number of the peaks identified. These were compared to patterns characteristic of specific bonds to determine if a unique spectrum for artemisinin derivatives could be identified using information from the following online sources, Byrd J [16] and the Chemical Education Digital Library [17].

### **Incorporation of DHA into viable erythrocytes and its identification *in situ***

Enucleate Erythrocytes were used to pilot *in-vivo* detection, being a simple cell type, as well as relevant to the original use of the drugs. They were obtained from a finger-prick into 10ml phosphate buffered saline (PBS) and washed twice by centrifugation. The artemisinin derivatives ART, DHA and ARTE were used. 0.2g of each derivative was dissolved into 2ml of absolute ethanol. 20µl of each artemisinin stock solution was added to 2ml of Erythrocytes in PBS, 2ml was kept as control. These were incubated with the derivatives for 30 minutes in a cell culture incubator (37°C, 5% CO<sub>2</sub> in humidified air). They were then centrifuged at 1200g for 5 minutes. The supernatant was removed and the cells were re-suspended in PBS and re-centrifuged. The resulting pellet was used to prepare cytospin slides.

Labeled slides were wrapped in aluminium foil, shiny-side-out, and placed in a cytospin centrifuge (Cytospin 4, Thermo Scientific, UK). The Erythrocytes pellets were added to the sample inlets on the cytospin filter and centrifuged at 1000rpm for 5 minutes. Slides were air-dried before spectra were obtained by forcing the blood spots onto the diamond crystal of the FT-IR analyser. A background spectrum for the aluminium foil was subtracted. OMNIC software was then used to subtract the untreated Erythrocyte spectrum from spectra obtained from cells treated with each artemisinin derivative. This provided three subtraction spectra with which to search against online

libraries.

### **Cytotoxicity to epithelial monolayers**

Cytotoxicity studies were performed according to the protocols used in previous studies from the group and set out in detail elsewhere [18]. Briefly, cells were seeded into 96-well plates, allowed to attach for 24 hours, treated with serial dilutions of drug, incubated further for 48 hours and the residual viable biomass assessed by the addition of 3-(4,5-Dimethylthiazol-2-yl)-2,5-Diphenyltetrazolium Bromide (MTT) reagent for 2 hours before measuring absorbance at 470nm on a plate-reading spectrophotometer.

### **Statistical analysis**

Statistical analyses were performed using SPSS software (version 19.0 for Windows; SPSS Inc., Chicago, Illinois, USA). Data were normally distributed, thus descriptive statistics are expressed as mean  $\pm$  standard errors of the mean. Data was subjected to a one-way analysis of variance (ANOVA), providing an overall figure of significance. In order to ascertain where the differences are and discover trends *post hoc* analysis the Tukey or Games-Howell tests were applied. The conventional  $p < 0.05$  value was used as the cut-off for significance.

## RESULTS

### In vitro results on raw materials

The first spectrum obtained for DHA is shown in figure 1. The very large peak at  $\sim 2450\text{cm}^{-1}$  can be ignored as being carbon dioxide interference from the atmosphere. This peak has been blanked out in subsequent spectra. The peak at  $3245\text{cm}^{-1}$  corresponds to the O-H bond within the DHA molecule, which is added to native artemisinin to form DHA and improve the solubility of the drug. The peak at  $2921.95\text{cm}^{-1}$  corresponds to C-H bonding. There is a peak at  $1750\text{cm}^{-1}$  that corresponds to a carbonyl C=O bond indicative of an aldehyde, amide, carboxylic acid or ester. Within the fingerprint region there are peaks between  $180$  and  $1300\text{cm}^{-1}$ , these correspond to the ether, C-O-C bonds within the molecule.

A new spectrum was obtained for DHA 52 days after the first; changes had occurred as shown in figure 2. The OH region became broader and formed a doublet, usually seen when a molecule contains both O-H and N-H bonding, which DHA should not. This change is indicative of degradation and may be due to moisture reacting with the O-H bonds during storage. Spectra for ART and ARTE were subsequently also obtained 14 days later (Day 66). They do not display such differences. Sample spectra are shown in figures 3 and 4.

Figure 3 consists of two spectra for ART taken eight weeks apart. The spectra do not have the degree of change seen with the DHA. There is some change in the C-H bond section just under  $3000\text{cm}^{-1}$ . ART was synthesised to be more water soluble and has a carboxylic acid group, corresponding peaks seen at  $1142/1144.53\text{cm}^{-1}$ , an additional ether C-O-C bond (smaller peaks between  $1080$  and  $1300\text{cm}^{-1}$ ), plus an ester bond O=C-O.

ARTE plots show little change with time (Figure 4). ARTE is a lipophilic alkylether without an OH group, so there is no peak between  $3200$  and  $3600\text{cm}^{-1}$ . There is a large peak that corresponds to C-H bonding between  $2850$  and  $3000\text{cm}^{-1}$ . ARTE does not have a carbonyl C=O bond therefore there is no peak between  $1690$ - $1760\text{cm}^{-1}$ . It has an additional methyl  $\text{CH}_3$  group; this may correspond to the peaks at  $1373/1372\text{cm}^{-1}$ , respectively. The  $\text{CH}_3$  is attached to an O, so there is a significant amount of C-O-C ether bonds, which can be seen in the peaks between  $1080$  and  $1300\text{cm}^{-1}$ .

OMNIC 6.1 software was used to confirm whether the DHA, ART and ARTE spectra matched spectra of molecules stored within online databases/libraries. Matches were not found, indicating their spectra are unique. A new library was set up containing the spectra for each of the artemisinin derivatives.

#### **Incorporation of DHA into viable erythrocytes and its identification *in situ***

For the ART and ARTE subtraction spectra, no strong matches were found. For the DHA treated cells a match of 80.87% with the spectra obtained after subtraction for the pure DHA compound (Figure 5).

#### **Cytotoxicity to epithelial monolayers**

All three artemisinin derivatives showed significant ( $P < 0.05$  vs control) toxicity studies using RTT112 bladder cancer cells in an MTT-based assay over  $1.5\mu\text{g/ml}$ , but the curves for ARTE were flatter than for ART or DHA with respective  $R^2$  values of 0.67, 0.74 and 0.96 (Figure 6). ARTE failed to achieve a reduction in residual viable biomass to 50% of control values ( $\text{IC}_{50}$ ) up to  $25\mu\text{g/ml}$ .  $\text{IC}_{50}$ s for ART and DHA were  $3\mu\text{g/ml}$  and  $9\mu\text{g/ml}$ , respectively.

## DISCUSSION

Semi-synthetic derivatives of the anti-malarial drug artemisinin may possess cytotoxic activity against nucleate cells growing *in vitro*, and anti-angiogenic activity [4,5], offering potential anti-cancer properties. To further the study of these phenomena the ability to detect artemisinin uptake and distribution in cells would be advantageous. Live cell imaging studies without the problems of labelling small molecules could be achieved through FT-IR spectroscopy. This study describes mid-range infrared absorption spectra for three artemisinin variants and detects the presence of one, DHA, in erythrocytes incubated with the drugs, albeit at this stage without imaging. It also assesses the cytotoxic effect of artemisinin derivatives in the RT112 bladder carcinoma cell line.

The structurally unique feature and key source of artemisinins activity is its endoperoxide bridge. However, as there is no net change in the dipole moment during the vibration of homonuclear molecules such as O<sub>2</sub>, N<sub>2</sub>, and H<sub>2</sub>, these molecules do not absorb IR radiation [19]. Therefore, the characteristic O-O bond within the endoperoxide bridge is unlikely to absorb IR and will not contribute a characteristic peak to the spectra for artemisinins. With that said, the spectra obtained still appeared to be unique and were not found within existing spectral databases. The 1750<sup>cm</sup>-1 C=O peak does not fit with the structure of DHA. Wild-type artemisinin does however have a C=O bond and this may suggest a level of impurity during the synthesis of DHA.

The Erythrocytes experiment indicated artemisinin derivatives spectra were potentially identifiable within a complex environment. The high dose used for this experiment is far in excess of those used elsewhere in the study or are attainable therapeutically, but follow a conventional progression in experimentation, starting with a strong effect that must be achievable for the system to show potential. Concentrations will subsequently be lowered to find threshold detection levels. The subtraction spectra of DHA in Erythrocytes achieved an 80.87% match with the spectrum for pure DHA, so some of the compound entered the cells remaining relatively unaltered. This may be due to a lack of free Fe<sup>2+</sup> within the 'normal' Erythrocytes. It is noteworthy that DHA was the most cytotoxic of the three derivatives towards RTT112 bladder cancer cells in log phase growth. For ART and ARTE no match was found, indicating that the compounds may not have entered the Erythrocytes at all, or had been modified beyond recognition by metabolic processes. The former possibility is arguably more likely, as Erythrocytes contain limited capacity for active metabolism.

Identifying the spectra of artemisinins within more metabolically active nucleate cells introduces several factors that require consideration and further study. Firstly, as the concentrations of the artemisinin derivatives present are far smaller and much harder to identify within a mixture, a range of different concentrations more closely approximating to clinically achievable plasma values than used here, should be applied to cells to assess the concentration limits for detection. Among the highest human plasma concentrations reported in the literature is 443ng/ml [20] compared with the 1mg/ml applied to the washed erythrocytes *in-vitro* here. Secondly, a range of cell lines could be used to demonstrate differences in uptake and detection. Thirdly, artemisinins are reactive, with a short half-life *in-vivo*. Oral artemisinins have been credited with a mean absorption time of 0.78 hours [21] and a residence time of 3.3hr. This compares unfavourably (32%) with bioavailability from intramuscular injection in oil. However, the mean residence time of the latter (10.6h) was three times longer than following oral administration. Gordi et al [22] quotes a half-life of 0.7h and hepatic extraction ratio of 0.87. When applying the derivatives to cells, key bonds may break (e.g., cleavage of the peroxide bridge) changing the molecular structure and altering the absorbance spectrum. Time series during exposure of live cells to drug may yield information on turnover as we have shown using time-lapse fluorescence in other contexts [23]. It may also with artemisinins, in the first instance be possible to tag the derivatives with a fluorochrome to allow parallel detection through fluorescent microscopy, adding validity to the images from a well-established method. Of course, the handling of a compound may be influenced by the label; circumventing that issue is an important driver towards IR imaging.

Uptake in erythrocytes is a first step towards detection in tissues and ultimately live cells. In this study it has already thrown up differences in detectability between the three variants used. There are also variations in cytotoxicity against RT112 cells, with artemether proving markedly less toxic. The focus on bladder cancer reflects the interests of our group, but as noted in the introduction, activity against other cancer cells has been demonstrated (4,5). Investigating the uptake and processing of artemisinins within cancer cells is therefore worthy of study and would ideally involve applying live cell imaging techniques [24] to provide valuable information in real time, particularly if rapid acquisition is possible using limited spectral information -for example on a QCL-based instrument [25].

#### **TAKE-HOME MESSAGE**

This first demonstration that DHA uptake can be detected by its presence in erythrocytes using FT-

IR spectroscopy, offers the possibility of localising the drug in fixed or potentially live cells without labelling, using IR imaging equipment. The failure to detect the other analogues may indicate their speedy intracellular metabolism and might shed light on the differences in cytotoxicity that clearly exist between the analogues, at least to the RT112 cell line *in-vitro*.

#### **LICENCE FOR PUBLICATION**

The Corresponding Author has the right to grant on behalf of all authors and does grant on behalf of all authors, an exclusive licence (or non-exclusive for government employees) on a worldwide basis to the BMJ Publishing Group Ltd to permit this article (if accepted) to be published in JCP and any other BMJPGJ products and sublicences such use and exploit all subsidiary rights, as set out in our licence (<http://group.bmj.com/products/journals/instructions-for-authors/licence-forms>).

#### **COMPETING INTEREST**

None declared.

#### **FUNDING**

The study was funded internally.

## REFERENCES

1. Meshnick SR. Artemisinin: mechanisms of action, resistance and toxicity. *Int J Parasitol* 2002;32(13):1655-60.
2. Scott MD, Meshnick SR, Williams RA, Chiu DT, Pan HC, Lubin BH, et al. Qinghaosu-mediated oxidation in normal and abnormal erythrocytes. *J Lab Clin Med* 1989;114(4):401-6.
3. Meshnick SR. The mode of action of antimalarial endoperoxides. *Trans R Soc Trop Med Hyg* 1994;88 Suppl 1:S31-2.
4. Fishwick J, McLean WG, Edwards G, Ward SA. The toxicity of artemisinin and related compounds on neuronal and glial cells in culture. *Chem Biol Interact* 1995;96(3):263-71.
5. Efferth T, Dunstan H, Sauerbrey A, Miyachi H, Chitambar CR. The anti-malarial artesunate is also active against cancer. *Int J Oncol* 2001;18(4):767-73.
6. Morrissey C, Gallis B, Solazzi JW, Kim BJ, Gulati R, Vakar-Lopez F, et al. Effect of artemisinin derivatives on apoptosis and cell cycle in prostate cancer cells. *Anticancer Drugs* 2010;21(4):423-32.
7. Zhou HJ, Wang WQ, Wu GD, Lee J, Li A. Artesunate inhibits angiogenesis and downregulates vascular endothelial growth factor expression in chronic myeloid leukemia K562 cells. *Vascul Pharmacol* 2007;47(2-3):131-8.
8. Aftab T, Khan MM, Idrees M, Naeem M, Moinuddin, Hashmi N. Methyl jasmonate counteracts boron toxicity by preventing oxidative stress and regulating antioxidant enzyme activities and artemisinin biosynthesis in *Artemisia annua* L. *Protoplasma* 2011;248(3):601-12.
9. Cai X, You P, Cai J, Yang X, Chen Q, Huang F. ART-induced biophysical and biochemical alterations of Jurkat cell membrane. *Micron* 2011;42(1):17-28.
10. Zhang X, Ba Q, Gu Z, Guo D, Zhou Y, Xu Y, et al. Fluorescent Coumarin-Artemisinin Conjugates as Mitochondria-Targeting Theranostic Probes for Enhanced Anticancer Activities. *Chemistry* 2015.
11. Yang ND, Tan SH, Ng S, Shi Y, Zhou J, Tan KS, et al. Artesunate induces cell death in human cancer cells via enhancing lysosomal function and lysosomal degradation of ferritin. *J Biol Chem* 2014;289(48):33425-41.
12. Xiao F, Gao W, Wang X, Chen T. Amplification activation loop between caspase-8 and -9 dominates artemisinin-induced apoptosis of ASTC-a-1 cells. *Apoptosis* 2012;17(6):600-11.
13. Gao W, Xiao F, Wang X, Chen T. Artemisinin induces A549 cell apoptosis dominantly via a reactive oxygen species-mediated amplification activation loop among caspase-9, -8 and -3. *Apoptosis* 2013;18(10):1201-13.

14. Ganguli A, Choudhury D, Datta S, Bhattacharya S, Chakrabarti G. Inhibition of autophagy by chloroquine potentiates synergistically anti-cancer property of artemisinin by promoting ROS dependent apoptosis. *Biochimie* 2014;107 Pt B:338-49.
15. Brown G. Artemisinin and a new generation of antimalarial drugs, 2006.
16. Byrd J. Characteristic infrared absorption frequencies. Retrieved 4 March, 2016 from: <http://wwwchem.csustan.edu/Tutorials/INFRARED.HTM>
17. Chemical Education Digital Library. Retrieved 4 March, 2016 from: <http://chempaths.chemeddl.org/services/chempaths?>
18. Jennings AM, Solomon LZ, Sharpe P, Hayes MC, Cooper AJ, Birch BR. Estramustine reversal of resistance to intravesical epirubicin chemotherapy. *Eur Urol* 1999;35(4):327-35.
19. Sherban-Kline M. *Infrared Spectroscopy: A Key to Organic Structure.*, 2012.
20. Dien TK, de Vries PJ, Khanh NX, Koopmans R, Binh LN, Duc DD, et al. Effect of food intake on pharmacokinetics of oral artemisinin in healthy Vietnamese subjects. *Antimicrob Agents Chemother* 1997;41(5):1069-72.
21. Titulaer HA, Zuidema J, Kager PA, Wetsteyn JC, Lugt CB, Merkus FW. The pharmacokinetics of artemisinin after oral, intramuscular and rectal administration to volunteers. *J Pharm Pharmacol* 1990;42(11):810-3.
22. Gordi T, Xie R, Jusko WJ. Semi-mechanistic pharmacokinetic/pharmacodynamic modelling of the antimalarial effect of artemisinin. *Br J Clin Pharmacol* 2005;60(6):594-604.
23. Featherstone JM, Lwaleed BA, Speers AG, Hayes MC, Birch BR, Cooper AJ. Time-lapse live cell imaging and flow analysis of multidrug resistance reversal by verapamil in bladder cancer cell lines. *Urology* 2009;74(2):378-84.
24. Soh J, Chueng A, Adio A, Cooper AJ, Birch BR, Lwaleed BA. Fourier transform infrared spectroscopy imaging of live epithelial cancer cells under non-aqueous media. *J Clin Pathol* 2013;66(4):312-8.
25. Clemens G, Bird, B., Weida, M., Rowlette, J., Bakera, M. Quantum cascade laser-based mid-infrared spectrochemical imaging of tissues and biofluids. *Spectroscopy Europe* 2014;26:14 - 19.

## LEGENDS TO FIGURES

### **Figure 1: Original DHA spectrum (Day 0)**

FT-IR spectrum of DHA crystals on aluminium foil. The large peak at  $\sim 2450\text{cm}^{-1}$  is considered to be interference from carbon dioxide in the atmosphere and has been blanked out in subsequent spectra.

### **Figure 2: Spectra for DHA obtained on (Day 52)**

Considerable changes have occurred since Day 0, notably the OH region broadening into a doublet, indicating O-H and N-H bonding.

### **Figure 3: FT-IR absorption spectra for ART**

Two spectra are shown, obtained on Day 0 (upper) and the following Day 66 (lower). The Spectra do not have the degree of change seen with DHA. There is some change in the C-H bond section just under  $3000\text{cm}^{-1}$ .

### **Figure 4: The FT-IR absorption spectra for ARTE**

Two spectra, taken on Day 0 (upper) and the following Day 66 (lower). These show little change. ARTE is without an OH group or carbonyl bond, so there are no peaks between  $3200$  and  $3600\text{cm}^{-1}$  or  $1690$ - $1760\text{cm}^{-1}$ . It has an additional methyl  $\text{CH}_3$  group, perhaps corresponding to the peaks at  $1373/1372\text{cm}^{-1}$ .

### **Figure 5: Subtraction and library search spectra for RBCs treated with DHA**

Lower plot – spectrum from ART ex-vivo. Upper plot – subtraction of erythrocyte spectrum from DHA-loaded erythrocytes.

### **Figure 6: Toxicity of DHA, ART and ARTE to RT112 cells**

MTT assay: Residual Viable Biomass as % control ( $\text{OD experimental} / \text{OD control} \times 100$ ) plotted as means  $\pm$ SEM (n=8) against concentration of drug.

Figure 1:

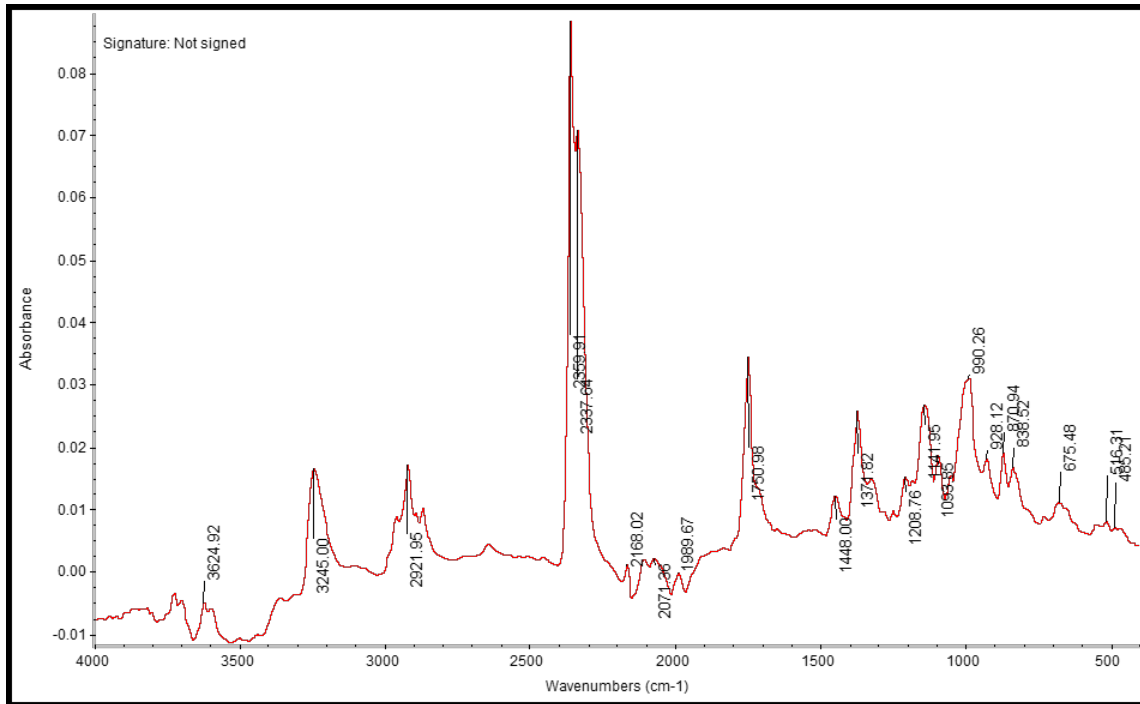


Figure 2:

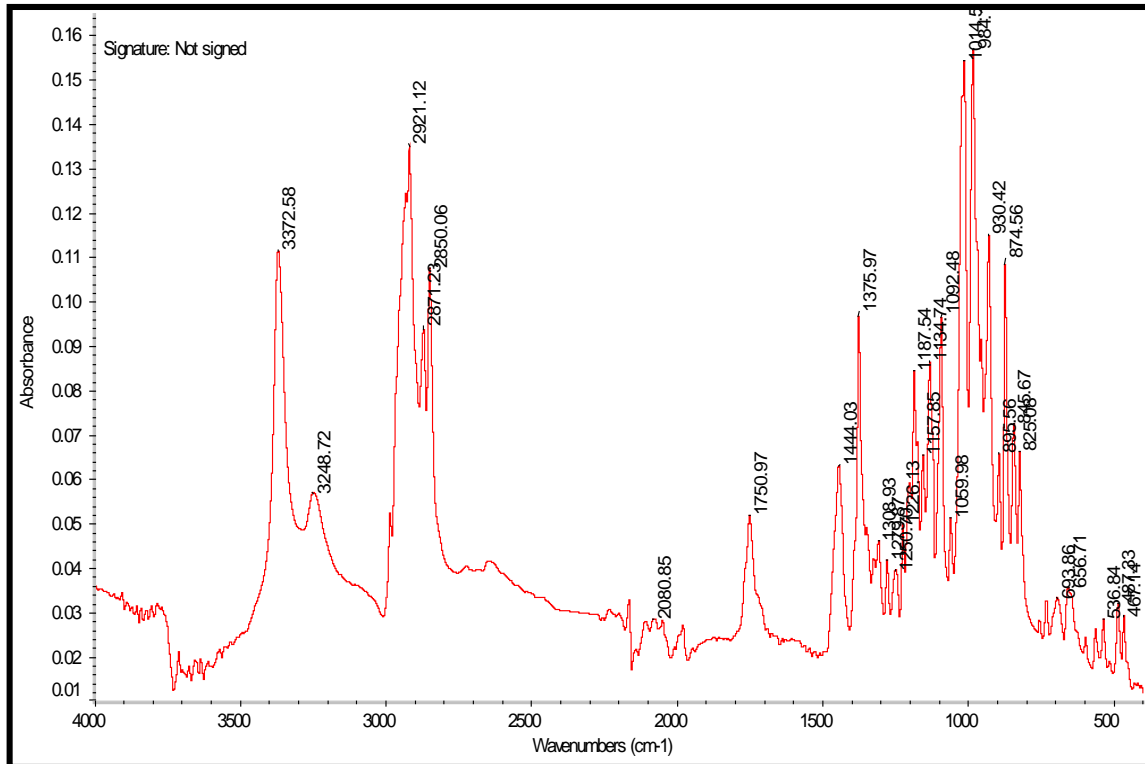


Figure 3:

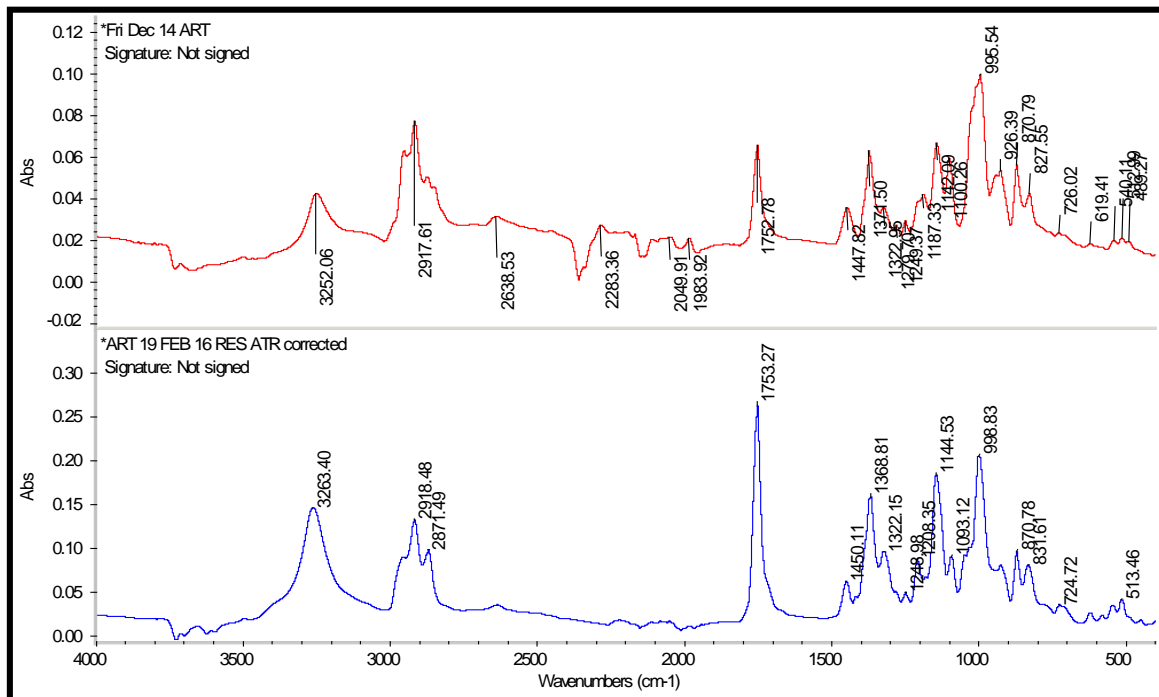


Figure 4:

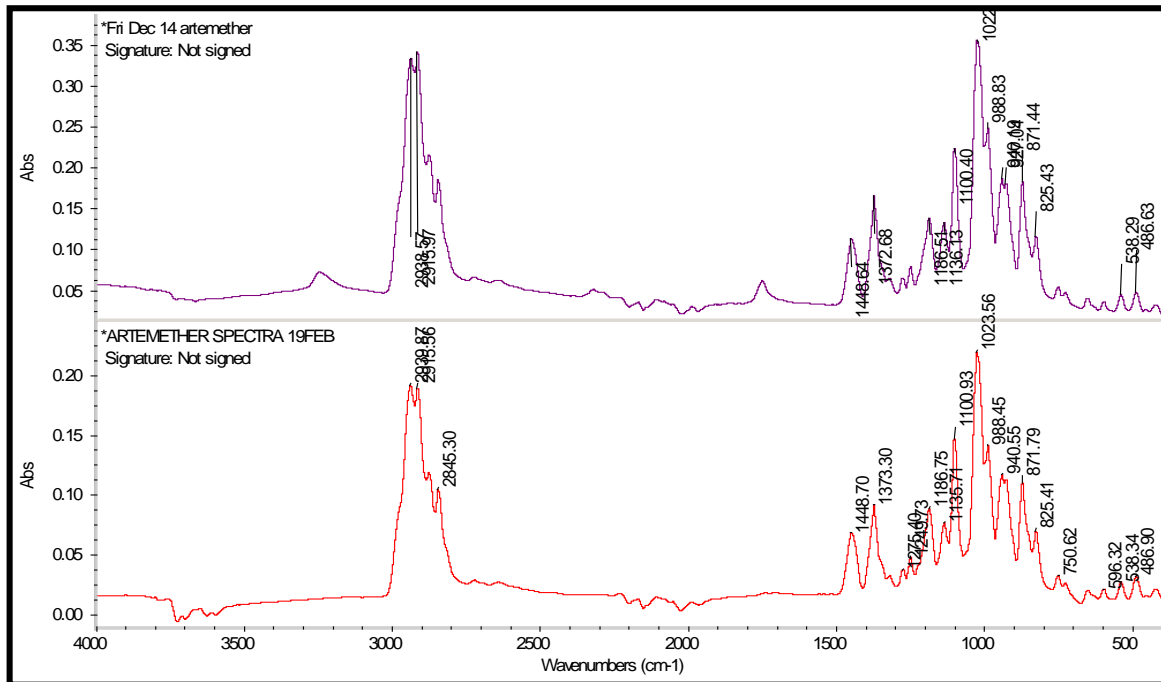


Figure 5:

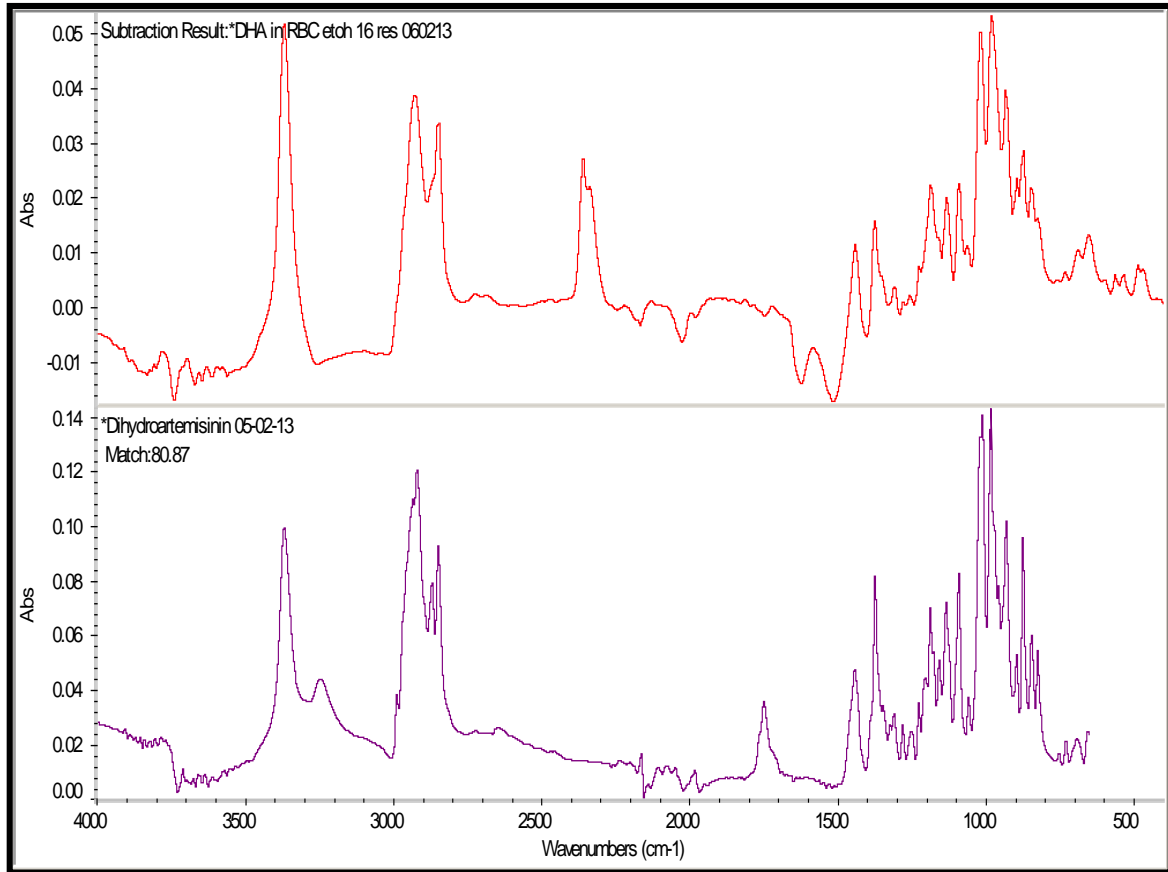


Figure 6:

